Frost, Ray L. and Shen, Wei and He, Hongping and Zhu, Jianxi and Yuan, Peng (2007) Grafting of montmorillonite with different functional silanes via two different reaction systems. *Journal of Colloid and Interface Science* 313(1):pp. 268-273.

Grafting of montmorillonite with different functional silanes via two different reaction systems

Wei Shen [a,c], Hongping He [a,b *], Jianxi Zhu [a], Peng Yuan [a], Ray L. Frost [b *]

[a] Guangzhou Institute of Geochemistry, Chinese Academy of Sciences, Guangzhou 510640, China

[b] Inorganic Materials Research Program, School of Physical and Chemical Sciences, Queensland University of Technology, GPO Box 2434, Brisbane, QLD 4001, Australia

[c] Graduate University of Chinese Academy of Sciences, Beijing 100039, China

[*] Corresponding authors: hehp@gig.ac.cn; r.frost@qut.edu.au

Abstract

Silane grafted montmorillonites were synthesized by using 3-aminopropyltriethoxysilane and trimethylchlorosilane via two different grafting reaction systems: (a) ethanol-water mixture and (b) vapour of silane. The resulting products were investigated using Fourier transform infrared (FTIR), X-ray diffraction (XRD), thermogravimetric analysis (TGA). XRD patterns demonstrate that silane was intercalated into the montmorillonite gallery, as indicated by the increase of the basal spacing. The product prepared by vapor deposition has a larger basal spacing than that obtained from solution, due to the different extent of silane hydrolysis in various grafting systems. TGA curves indicate that the methyl groups penetrate into the siloxane clay are the primary reason for the decrease of the dehydroxylation temperature of the grafted products. 3-aminopropyltriethoxysilane in the grafted montmorillonite adopts a bilayer arrangement while trimethylchlorosilane adopts a monolayer arrangement within the clay gallery.

Keywords: Montmorillonite; Grafting; 3-aminopropyltriethoxysilane; Trimethylchlorosilane;

Fourier transform infrared; X-ray diffraction; Thermogravimetric analysis

1. Introduction

Expandable clay minerals such as smectites have extensive applications in various fields due to its swelling behavior, adsorption properties, ion exchange property and high surface areas [1-5]. The most commonly used swelling clay is the dioctahedral clay: montmorillonite, which has two siloxane tetrahedral sheets sandwiching an aluminum octahedral sheet. Due to isomorphic substitution within the layers (for example, Al^{3+} replaced by Mg^{2+} or Fe^{2+} in the octahedral sheet; Si^{4+} replaced by Al^{3+} in the tetrahedral sheet), the clay layer is negatively charged, which is counterbalanced by the cations within the interlayer space. The hydration of inorganic cations on the exchange sites causes its surface to be hydrophilic. Thus it is difficult for some organic molecules to be intercalated into montmorillonite by conventional ion exchange methods because of the highly hydrophobia and bulk of the organic molecules. Recently, their potentials have been greatly expanded by being grafted with a variety of biologically active organic substances [6-9]. Hydrophobic modification of the clay intra-surface allows many hydrophobic guest molecules to be readily intercalated.

As is well known, there are various ways to modify clay minerals, i.e., adsorption, ion exchange with organic/inorganic cations, grafting with organic compounds [10]. Organoclays are usually synthesized by modifying clays with surfactants via ion exchange [11, 12]. In this way the hydrophobic partition medium within the clay interlayer can be formed and functions analogously to a bulk organic phase. The organoclays can be used to remove toxic compounds from the environment and reduce the dispersion of pollutants in soil, water, and air. In the organoclays, the cationic surfactant is fixed by the electrostatic force and may be released in the aqueous medium [13], resulting in secondary pollution. However, in the case of silane grafted clays, the organic molecule is tightly bonded onto the clay surface by the condensation between silane and clay minerals. Thus the release of the organic molecule into the aqueous medium is excluded. The silane grafted clays will be useful in the fields of remediation of polluted environments.

Previous studies have detailed the effects on the grafted products resulting from the used clay materials and silylating agents [14, 15]. Less attention was paid to the effects from the grafting methods and media. The main objective of this work is to elucidate the possible variations resulting from different preparation methods. In the present work, two different silanes (3-aminopropyltriethoxysilane and trimethylchlorosilane) were used and two different reaction systems were employed. In the first method, the grafting reaction was carried out in a mixture of ethanol/water while the second method is exposing Na-MMT samples to saturated vapor from refluxing silane. The resultant products were characterized by FTIR, XRD, and TGA, providing some new insights about structure of silane grafted clays and the effects from the various grafting ways. This is of high importance for synthesis and application for silane grafted clays.

2. Experimental

2.1. Materials

The swelling clay used in this work is a montmorillonite (Ca-MT), provided by Nanhai Mining Ltd., China. The cation exchange capacity (CEC) of montmorillonite is 60 meq/100 g. The structural formula of Ca-Mt can be expressed as $(Na_{0.009}Ca_{0.193}Mg_{0.064})(Fe_{0.086}Mg_{0.475}Al_{1.440})(Si_{3.96}Al_{0.04})O_{10}(OH)_{10} \bullet nH_2O$, deduced from the chemical analysis result.

The silanes used in this research are 3-aminopropyltriethoxysilane (γ -APS, with a purity of 99%, from Aldrich) and trimethylchlorosilane (TMCS, with a purity of 98%, from Sinopharm Chemical Reagent Co., Ltd). Both silanes were used as received without any further purification. Fig. 1 shows the schematic of the used silanes.

2.2. Preparation of sodium exchanged montmorillonite

In the preparation of Na-Mt, 10 g of the mixture of Ca-Mt (9.4 g) and Na_2CO_3 (0.6 g) was added into 100 ml of deionized water and stirred at 80 ^oC for 3 h. Na-Mt was collected by centrifugation and washed with deionized water. The Na-Mt was dried at 105 ^oC, ground and sieved through 200 mesh and then placed in a bottle and sealed for further use.

2.3. Grafting methods

In the present study, two different grafting methods were used. One is that the grafting reaction was carried out in a mixture of ethanol/water (75/25 by volume). Na-MMT (2.5 g) was firstly dispersed in a mixture solution (200 ml), and then 2 g of γ –APS was introduced into the above-mentioned mixture and sheared for 8 h at 80 ^oC. The resultant product was washed using the mixture of ethanol/water in order to remove the residual silane and dried at 60 ^oC in a vacuum oven. The product of γ –APS grafted montmorillonite prepared using the above-mentioned method was denoted as M-APS-1. Similarly, the product prepared from TMCS is marked as M-TMCS-1.

The second method for grafting reaction was carried out by exposing Na-MMT samples to saturated vapor from refluxing silane (γ –APS and TMCS, respectively) for 6 h. The temperature was maintained at the boiling point of the used silane. The grafted products were washed with ethanol to remove the residual silane and evacuated at 60 ^oC. The grafted montmorillonites were denoted as M-APS-2 and M-TMCS-2, respectively.

2.5. Characterization

Fourier transform infrared (FTIR) spectra using the KBr pressed disk technique were performed on a Bruker Vector 33 Fourier transform infrared spectrometer. 32 scans were collected for each measurement over the spectral range of 400–4000 cm^{-1}

with a nominal resolution of 4 cm^{-1}.

X-ray diffraction (XRD) patterns were obtained using Bede D1 system diffractometer (Cu K_α radiation under target voltage of 35 kV and current of 30 mA, λ= 0.154 nm). The basal spacings were calculated from the 2θ values using the EVA software.

Thermogravimetric analysis (TG) of montmorillonite and the grafted products were performed on a TG209 thermobalance. Samples were heated from 30 to 900 ^oC at ramp 15 ^oC /min under a N_2 flow (25 mL/min) to quantify and distinguish the amount of silane in the grafting products.

3. Results and discussion

3.1. Powder X-ray diffraction

With grafting silane onto montmorillonite, the expansion of the montmorillonite layers was demonstrated by X-ray diffraction. The XRD patterns of the montmorillonite before and after grafting are shown in Figs. 2 and 3. The basal spacing for the Na-MMT is 1.26 nm, the characteristic d(001) value of sodium montmorillonite as reported in literature [15, 16]. As shown by the XRD patterns, the basal spacings of the silane grafted montmorillonites are obviously bigger than that of Na-MMT, indicating that the silane has been intercalated into montmorillonite interlayer space. After the grafting reaction, the basal spacing increased to 1.47 nm for M-TMCS-1 and to 1.56 nm for M-TMCS-2 (Fig. 2). Fig. 3 clearly shows an increase of the basal spacing from 1.26 nm for Na-MMT to 1.95 nm for M-APS-1 and to 1.98 nm for M-APS-2. Here, it can be found that both the grafting method and the used silanes have effects on the interlayer structure of the grafting products. In other words, in the case of grafting reaction carried out by exposing Na-MMT samples to saturated vapor from refluxing silane, the silane grafted montmorillonites have a bigger basal spacing than those prepared from the mixture of ethanol and water. Also, the configuration of the silane has a prominent effect on the interlayer height of the grafted montmorillonites. The configuration of γ –APS is different from that of TMCS. The height of the aminopropyl group in γ –APS is ca. 0.46 nm, similar to that of the alkyl chain, while the height of the Si bonding with three methyl groups in TMCS is ca. 0.51 nm, similar to that of the “nailhead” of the cationic surfactant (hexadecyltrimethylammonium bromide) [17]. The estimated gallery heights for M-TMCS-1 and M-TMCS-2 are 0.51 nm and 0.6 nm, deduced from the basal spacings and the height of montmorillonite. The gallery heights for M-APS-1 and M-APS-2 are 0.99 nm and 1.02 nm, respectively. It is proposed that the monolayer and bilayer arrangement models are adopted for TMCS and APS within the montmorillonite gallery [18]. As we know, in the solution of ethanol/water mixture, silane is easy to hydrolyze and condensate among silane molecules [19]. After hydrolysis, the configuration of silane will be changed with polymerization [15]. The hydrolyzed silane molecules can combine by means of condensation reaction to form

a siloxane linkage as following reactions (1a and 1b) [20].

$\equiv Si\text{-}OEt + H_2O \rightarrow \equiv Si\text{-}OH + EtOH$ (1a)

$\equiv Si\text{-}OH + OH\text{-}Si\equiv \rightarrow \equiv Si\text{-}O\text{-}Si\equiv + H_2O$ (1b)

In the case of the mixture of ethanol and water, it is likely that hydrolysis and condensation occurs before intercalation [21]. With the hydrolysis and polymerization, different polymers with various sizes can be formed, such as linear, monocyclic, polycyclic and 'cagelike', depending on the water amount in the reaction system [22]. Hence, polymerization results in the difficulty for the intercalation and only those with appropriate size and configuration (i.e. linear configuration) can be intercalated into the gallery of the montmorillonite. Upon grafting the montmorillonite by exposing to the saturated vapor from the refluxing silane, the single silane molecules were intercalated into the montmorillonite interlayer space and the basal spacing is a function of the amount of the intercalated organic molecules, similar to that intercalating surfactant into clay gallery. Then, the hydrolysis and condensation of silane takes place. In this case, more silane will be intercalated into the clay gallery, compared with the case of preparation in the mixture of ethanol and water. This proposal is supported by the TG and FTIR evidences.

3.2. FTIR analysis

The successful grafting is evident in the infrared spectra as shown in Figs. 4 and 5. The peak at 3623 cm^{-1} corresponds to the hydroxyl stretching vibration attributed to the OH units bonded to the aluminium and/or magnesium in Na-MMT. The peak at ca. 3433 cm^{-1} corresponds to the –OH stretching vibration of the adsorbed water [23].

In Fig. 4, a new peak at 2964 cm^{-1} attributed to antisymmetric stretching of $–CH_3$ group of TMCS was observed, indicating the existence of silane in the grafted products. This peak in the spectrum of M-TMCS-1 is very weak (see the magnified part in Fig. 4) but prominent in that of M-TMCS-2. This suggests that there are more silane in M-TMCS-2 than that in M-TMCS-1. Similarly, the intensities of the bands at 2926 and 2854 cm^{-1}, corresponding to the antisymmetric and symmetric stretching vibrations of $–CH_2$, increase from M-APS-1 to M-APS-2 (Fig. 5), implying an increase of the grafted γ –APS. Here, it can be seen that the grafting method has an important influence on the amount of the grafted silanes, i.e., the grafting reaction conducted in the silane vapor favors silane entering into the clay interlayer.

3.3. Thermal analysis of grafted montmorillonite

Thermogravimetric analysis (TGA) was provided as a simple method to measure the content of silanes and physisorbed water [24]. This method is based on the assumption that the dehydration and dehydroxylation reactions correspond to the two discrete mass loss steps in TG curves and they do not overlap each other [24]. The decomposition of silane grafted montmorillonite can be separated into 6 steps in this study and their corresponding mass losses are reported in Table 1. The thermogravimetric analysis of the pure montmorillonite is shown in Fig. 6. The DTG

curve of Na-MMT displays two peaks at ca. 56 and 639 ^{o}C, assigned to the loss of the physically adsorbed water and the dehydroxylation of montmorillonite [25]. For Na-MMT, there is a small mass loss (ca. 0.98%) in the range 150–440 ^{o}C, attributed to the loss of the bonded H_2O within the gallery. Therefore, a greater mass loss than expected is attributed to the evaporation and decomposition of silane.

The DTG curve of M-TMCS-1 displays three peaks at 66, 130 and 626 ^{o}C, respectively. The shoulder at 130 ^{o}C, with a mass loss of 0.88%, is attributed to the evaporation/decomposition of intercalated silane. The mass loss corresponding to the peak at ca. 66 ^{o}C is about 9.35%, obviously bigger than that of Na-MMT (6.68%). The boiling point of TMCS is 57.6 ^{o}C. This suggests that the mass loss at ca. 66 ^{o}C results from the physically adsorbed water/physically adsorbed silane. Also, a slight decease of the dehydroxylation temperature of montmorillonite was observed. The DTG curve of M-TMCS-2 shows three peaks at 64, 134 and 552 ^{o}C, and the peak at 134 ^{o}C with a mass loss of 2.84% is attributed to the mass lost of intercalated silane. And the dehydroxylation temperature of montmorillonite moves to 552 ^{o}C, which is more significant than that observed in M-TMCS-1. In the study of surfactant modified clays, similar phenomenon has been observed and it was attributed to the penetration of the methyl groups of the intercalated surfactant into the siloxane layer [26]. The more significant dehydroxylation temperature decrease in M-TMCS-2 than that in M-TMCS-1 should be attributed the larger amount of the intercalated silane in the former as shown in Table 1.

The DTG curves of M-APS-1 and M-APS-2 are shown in Fig. 6. Five peaks are observed in M-APS-1. The peaks at 63 and 632 ^{o}C are attributed to the loss of the physically adsorbed water and dehydroxylation of montmorillonite. The peaks at 346 and 429 ^{o}C with a mass loss of 1.30 and 6.96% are attributed to the decomposition of the intercalated silane while the peak at 533 ^{o}C is corresponding to the decomposition of the grafted silane [15]. For the M-APS-2, the peaks of 328, 427 and 531 ^{o}C correspond to the decomposition of the intercalated silane and the decomposition of the grafted silane. An additional peak is recorded at 255 ^{o}C with a mass loss of 4.79%, attributed to desorption from the external surfaces [15]. It is noted that after grafting with γ –APS, the prominent peak at ca. 639 ^{o}C corresponding to the dehydroxylation of montmorillonite was clearly observed. This is very different from that reported in the literature [27].

4. Conclusions

In this study, silane grafted montmorillonites were synthesized with trifunctional silane (γ –APS) and monofunctional silane (TMCS) using the mixture of ethanol/water and under the silane vapor. The basal spacings of the silane grafted montmorillonites are significantly larger than that of Na-MMT. This indicates that the silane has been intercalated into montmorillonite interlayer space. However, the configuration of the silane has a prominent effect on the interlayer structure and

consequential interlayer spacing. Our study demonstrates that the grafting reaction from the silane vapor favors silane entering into the clay interlayer as compared with the use of a mixture of ethanol and water. These suggestions were evidenced by the intensity increase of the antisymmetric stretching mode of $–CH_3$ in TMCS, and antisymmetric and symmetric stretching vibrations of $–CH_2$ in γ –APS. DTG results provide further supporting evidence for the grafting of the silane. The penetration of methyl groups into the hexagonal cavities of clay may be the primary reason for resulting in the dehydroxylation temperature decrease of montmorillonite, similar to that about surfactant intercalated montmorillonites reported in previous studies. Further work is currently underway using the molecular simulation and ^{13}C and ^{29}Si MAS NMR spectra.

Acknowledgments

This work was financially supported by the grant of the Knowledge Innovation Program of the Chinese Academy of Sciences (Grant No. Kzcx2-yw-112) and the National Natural Science Foundation of China (Grant No. 40572023).

References

[1] G. R. Alther, Contam. Soils 8 (2003) 189.

[2] G. R. Alther, Spec. Publ. R. Soc. Chem. 259 (2000) 277.

[3] C. Breen, R. Watson, J. Madejova, P. Komadel, Z. Klapyta, Langmuir 13 (1997) 6473.

[4] S. K. Dentel, J. Y. Bottero, K. Khatib, H. Demougeot, J. P. Duguet, C. Anselme, Water Res. 29 (1995) 1273.

[5] H. P. He, J. G. Guo, X. D. Xie, J. L. Peng, Environ. Int. 26 (2001) 347.

[6] G. Lagaly, Clay Miner. 16 (1981) 1.

[7] R. A. Vaia, R. K. Teukolsky, E. P. Giannelis, Chem. Mater. 6 (1994) 1017.

[8] L. P. Meier, R. Nueesch, F. T. Madsen, J. Colloid Interface Sci. 238 (2001) 24.

[9] H. P. He, R. L. Frost, F. Deng, J. X. Zhu, X. Y. Weng, P. Yuan, Clay Clay Miner. 52 (2004) 350.

[10] F. Bergaya, G. Lagaly, Applied Clay Science. 19 (2001) 1

[11] N. M. Soule, S. E. Burns, J. Geotech. Geoenviron. Eng. 127 (2001) 363.

[12] M. M. Mortland, S. Shaobai, S. A. Boyd, Clays Clay Miner. 34 (1986) 581.

[13] H. P. He, J. Duchet, J. Galy, J. F. Gerard, J. Colloid Interface Sci. 295 (2006) 202.

[14] N. N. Herrera, J. M. Letoffe, J. L. Putaux, L. David, E. Bourgeat-Lami, Langmuir 20 (2004) 1564.

[15] H. P. He, J. Duchet, J. Galy, J. F. Gerard, J. Colloid Interface Sci. 288 (2005) 171.

[16] R. L. Frost, L. Rintoul, Applied Clay Sci. 11 (1996) 171.

[17] J. X. Zhu, H. P. He, J. G. Guo, D. Yang, X. D. Xie, Chin. Sci. Bull. 48 (2003) 368.

[18] H. P. He, J. Galy, J. F. Gerard, J. Phys. Chem. B 109 (2005) 13,301.

[19] S. Ek, E. I. Iiskola, L. Niinistö, J. Phys. Chem. B. 108 (2004) 11,454.

[20] C. J. Brinker and G. W. Scherer, Sol-Gel Science, The Physics and Chemistry of Sol-Gel Processing, Academic Press, London, 1990, p 97.

[21] J. Ahenach, P. Cool, E. Vansant, O. Lebedev, J. V. Landuyt, Phys. Chem. Chem. Phys. 1 (1999) 3703.

[22] M. M. Sprung, F. O. Guenther, J. Am. Chem. Soc. 77 (1955) 3996.

[23] R. L. Frost, J. T. Kloprogge, Spectrochimica Acta Part A 56 (2000) 2177.

[24] S. Ek, A. Root, M. Peussa, L. Niinistö, Thermochim. Acta 379 (2001) 201.

[25] R. L. Frost, H. Ruan, J. T. Kloprogge, W. P. Gates, Thermochimica Acta 346 (2000) 63.

[26] Q. Zhou, R. L. Frost, H. P. He, Y. F. Xi, J. Colloid Interface Sci. 307 (2007) 50.

[27] Y. F. Xi, Z. Ding, H. P. He, R. L. Frost, J. Colloid Interface Sci. 277 (2004) 116.

Table.1. The results and the mass loss of the DTG curves.

Sample name	First step	Second step	Third step	Fourth step	Fifth step	Sixth step
Na-MMT	56 °C 6.68%					639 °C 5.26%
M-TMCS-1	66 °C 9.35%	130 °C 0.88%				626 °C 2.58%
M-TMCS-2	64 °C 9.05%	134 °C 2.84%				552 °C 5.05%
M-APS-1	63 °C 3.39%		346 °C 1.30%	429 °C 6.96%	533 °C 0.80%	632 °C 3.22%
M-APS-2	63 °C 3.31%	255 °C 4.79%	328 °C 1.14%	427 °C 6.49%	531 °C 1.06%	631 °C 3.10%

List of Figures

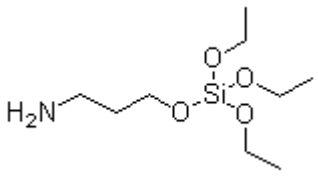

***γ* –APS**

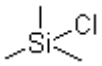

TMCS

Figure 1

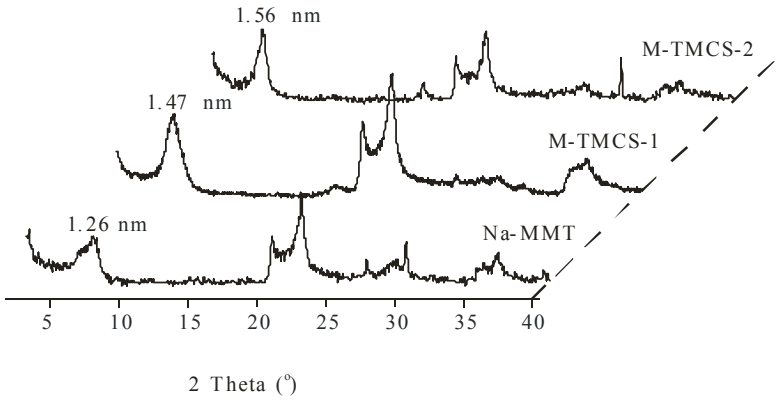
1.56 nm
M-TMCS-2
1.47 nm
M-TMCS-1
1.26 nm
Na-MMT
5
10
15
20
25
30
35
40
2 Theta (°)

Figure 2

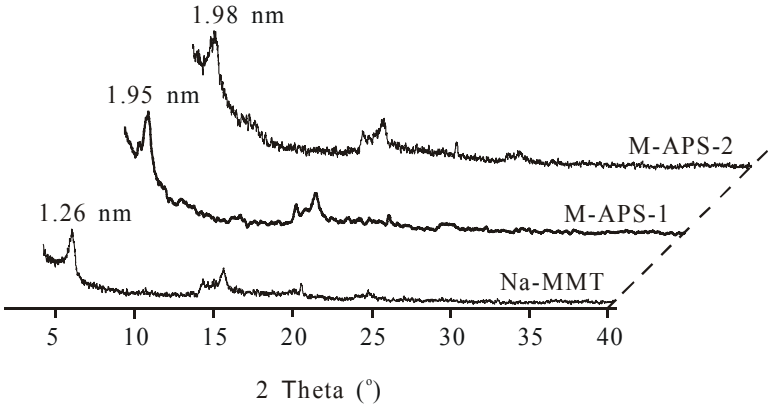
1.98 nm
1.95 nm
M-APS-2
1.26 nm
M-APS-1
Na-MMT
5
10
15
20
25
30
35
40
2 Theta (°)

Figure 3

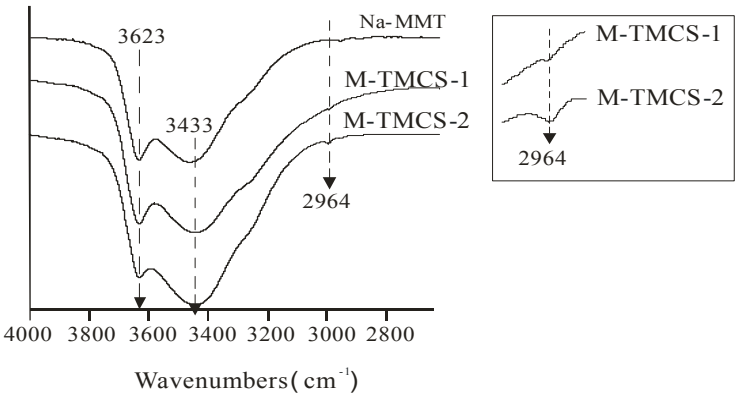
Na-MMT
3623
M-TMCS-1
3433
M-TMCS-2
2964
4000 3800 3600 3400 3200 3000 2800
Wavenumbers(cm-1)
M-TMCS-1
M-TMCS-2
2964

Figure 4

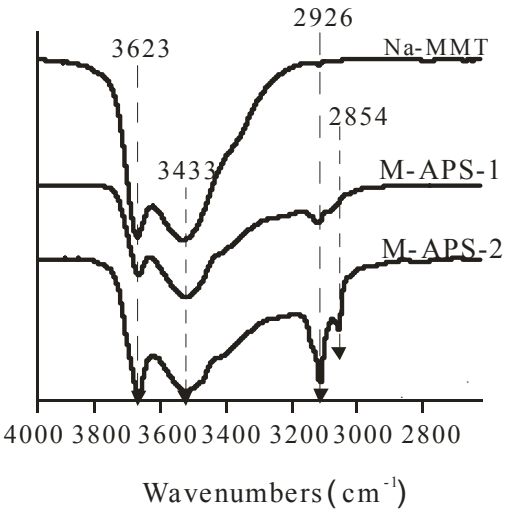
2926
3623
Na-MMT
2854
3433
M-APS-1
M-APS-2
4000 3800 3600 3400 3200 3000 2800
Wavenumbers (cm-1)

Figure 5

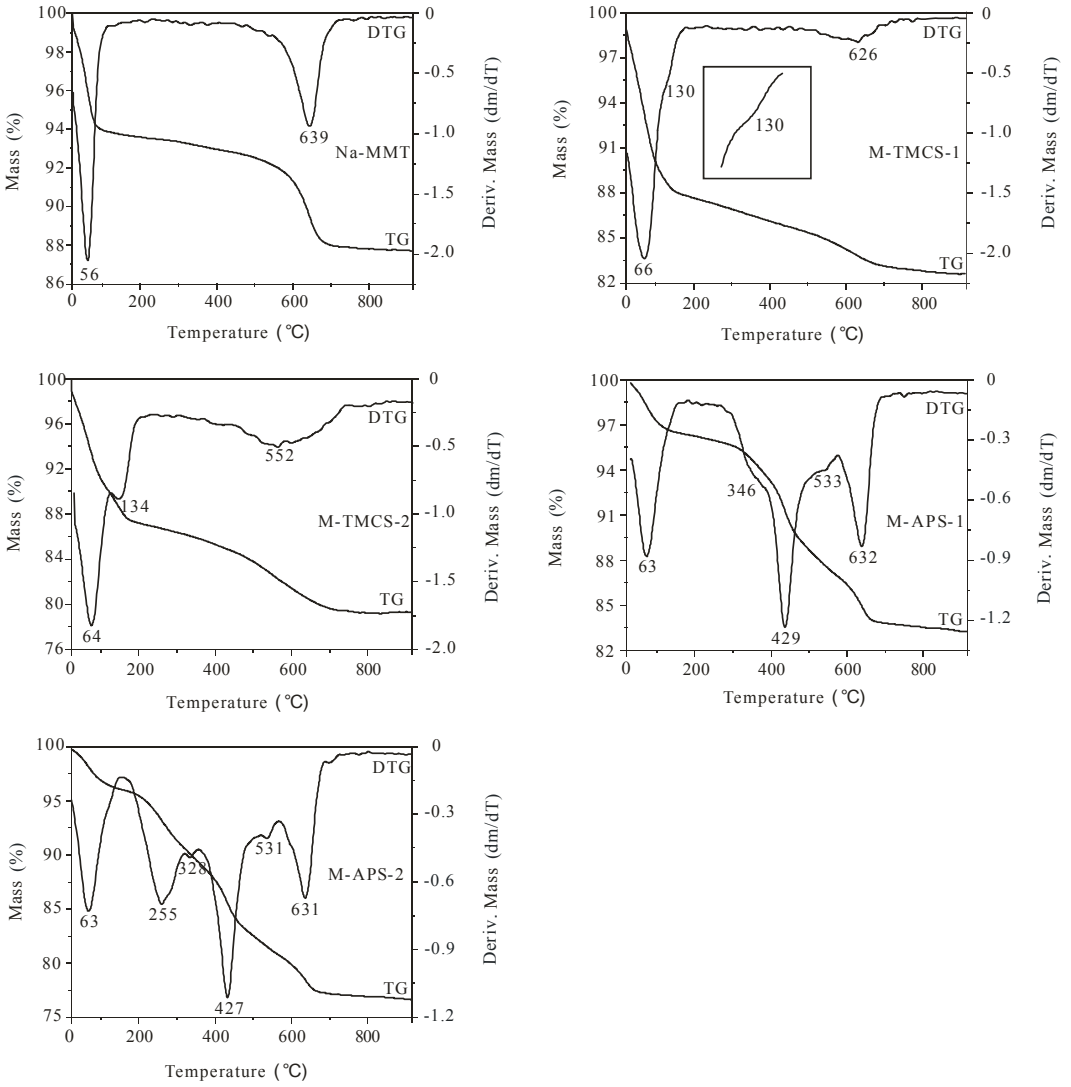
Mass (%)
Deriv. Mass (dm/dT)
Temperature (℃)
DTG
TG
Na-MMT
56
639
M-TMCS-1
66
130
626
M-TMCS-2
64
134
552
M-APS-1
63
346
533
429
632
M-APS-2
63
328
255
531
631
427

Figure 6